

Improved radar QPE with temporal interpolation using an advection scheme

Alrun Jasper-Tönnies¹ and Markus Jessen¹

¹hydro & meteo GmbH & Co, KG, Breite Str. 6-8, 23552 Lübeck, Germany

(Dated: 18 July 2014)



A. Jasper-Tönnies

1 Introduction

The temporal resolution of most European rain radars ranges from 5 min to 15 min. Also with a resolution of 5 min, the time gap between two measurements can lead to advection errors in radar rain sums. A significant improvement can be achieved by a temporal interpolation, based on an advection scheme as it is used for nowcasting. As a difference to nowcasting, advection can be determined more reliably as not only past radar measurements can be used for processing, but also subsequent measurements. Advection correction has been done by Ciach et al. (1997) and Anagnostou & Krajewski (1999) using cross-correlation to determine advection vectors.

Here we propose a temporal interpolation method that can also be conducted on a polar grid, keeping the original resolution of radar products without losing information by mapping and remapping rain intensity. It is therefore also appropriate as a correction step prior to rain gauge adjustment or producing radar composites.

An evaluation is done with one year data from radar Essen and measurements from 137 rain gauge stations.

2 Interpolation Method

From radar nowcasting, a number of methods are known to extrapolate radar intensities into the future. Most of these methods are also appropriate for a temporal interpolation between subsequent radar scans. Here we use an extrapolation method based on cell recognition which is a further development of a nowcast method described in Tessendorf et al. (2012) and included in the software package SCOUT (hydro & meteo, 2009). Polar radar data are mapped on a Cartesian grid with grid length 1km. With image analysis and pattern recognition, structures and rain cells (above flexibly adapted intensity thresholds) are detected and tracked. The identified advection vectors are interpolated to an advection field for the complete radar area. The advection of the intensity field on the grid is done using a Semi-Lagrange scheme. Enhancements compared to Tessendorf et al. (2012) are a filter substantially reducing diffusion on the grid as well as additional confidence criteria for the use of differing cell information. An example of the 1h-nowcast of the intensity field is shown in Figure 1.

When using the nowcast scheme for a temporal interpolation, several adaptations are made, as the initial position and the focus are slightly different from nowcasting:

1. To improve the QPE by temporal interpolation, mass conservation during the advection is important
2. The original spatial resolution from the polar radar scan should be kept without losing information by mapping and remapping the data
3. Compared to the nowcasting scheme, not only past information is available for the temporal interpolation but also future information. As the method should also be usable in a real-time environment a compromise is needed between fast availability and using all relevant data for interpolation.

2.1 Calculation of the advection field

We start with two subsequent radar scans measured at times t_{R1} and t_{R2} and aim to determine the rain in the intermediate time $t_i \in (t_{R1}, t_{R2})$. Radar rain rates $R(t_{R1})$ and $R(t_{R2})$ are derived using an appropriate ZR-Relation.

First step is to derive the advection field for the time t_i . This is done the same way as described above for nowcasting, recognising rain cells and structures and determining the advection vectors. The only difference is that a number of images up to t_{R2} instead of t_{R1} is used to derive the advection field. The field is assumed to be constant for t_i . In order to use algorithms for image analysis and cell recognition, the intensity fields are mapped to a Cartesian grid and the resulting advection field is first calculated on the Cartesian grid and then mapped to the original polar grid. As transitions are smooth in the advection field, this mapping step involves almost no loss of information.

2.2 Advection with the Lagrange scheme

The next step is the advection of the radar rain rates $R(t_{R1})$ and $R(t_{R2})$ on the polar grid. We sample the intermediate time $\Delta t_R = t_{R2} - t_{R1}$ with n steps $i = 1:n$, using a time interval of 1 min. A Lagrange scheme is used to calculate the advection of the rain field which is a difference to the nowcast algorithm, where a Semi-Lagrange scheme is used. Lagrange schemes are automatically mass-conserving while common disadvantages (e.g. potentially empty grid points) are not relevant in this context, due to the short time step and no need for continuous fields.

Every grid point with rain from $R(t_{R1})$ is assumed to be a parcel located at the grid point center. The advection vector at this place is used to calculate the new location of the parcel. There, a distance-weighted interpolation to the four neighbouring polar grid points is done. The advection is calculated separately for every time step, resulting in the rain rates $AR(t_{R1}, i)$, $i = 1:n$. Based on $R(t_{R2})$, advected rain rates $AR(t_{R2}, i)$ are calculated for each time step likewise, using the inverse advection field.

2.3 Interpolated rain rates

The radar rain rate $R(t_i)$ is calculated as weighted superposition of $AR(t_{R1}, i)$ and $AR(t_{R2}, i)$:

$$R(t_i) = w_1 \cdot AR(t_{R1}, i) + w_2 \cdot AR(t_{R2}, i) \quad (2.1)$$

where w_1 and w_2 are the weights depending on the time-lag with:

$$w_1 = \frac{n-i}{n}, w_2 = \frac{i}{n} \quad (2.2)$$

Close to the border of the radar circle, $AR(t_{R1}, i)$ or $AR(t_{R2}, i)$ may not be defined because the starting point of advection is outside the radar area. In this case the weights become $w = 0$ for the undefined and $w = 1$ for the defined advected rain to avoid a decrease of rain towards the border. The resulting mean rain rate for the period from t_{R1} to t_{R2} is:

$$\bar{R}(t_{R1}, t_{R2}) = \frac{1}{n} \sum_{i=1}^n R(t_i) \quad (2.3)$$

Depending on the further processing, it can be useful to choose a monotone ZR-Relation for determining the rain rates $R(t_{R1})$ and $R(t_{R2})$ and to transfer the interpolated rain rate $\bar{R}(t_{R1}, t_{R2})$ to a mean rain intensity in dBZ.

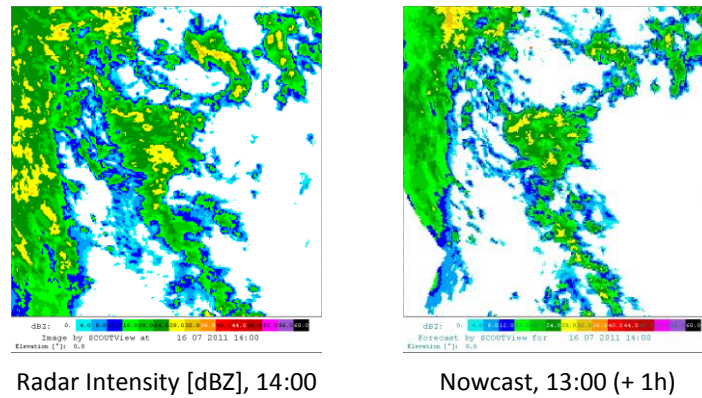


Figure 1: Rain intensity from radar measurement and 1h-Nowcast in a Dutch composite from the project HydroCity (Einfalt et al., 2012).

3 Evaluation Set-up

For the evaluation of the temporal interpolation method, polar radar data from the C-band radar Essen (DX product with resolutions 1 km x 1°, 5 min, 0.5 dBZ) operated by the German weather service were used. In addition, 137 rain gauges were available from the catchments of two water authorities, Emschergerenossenschaft/ Lippeverband and Bergisch-Rheinischer Wasserverband (see Figure 2). The time period of the investigation is one year from 1st November 2007 – 1st November 2008.

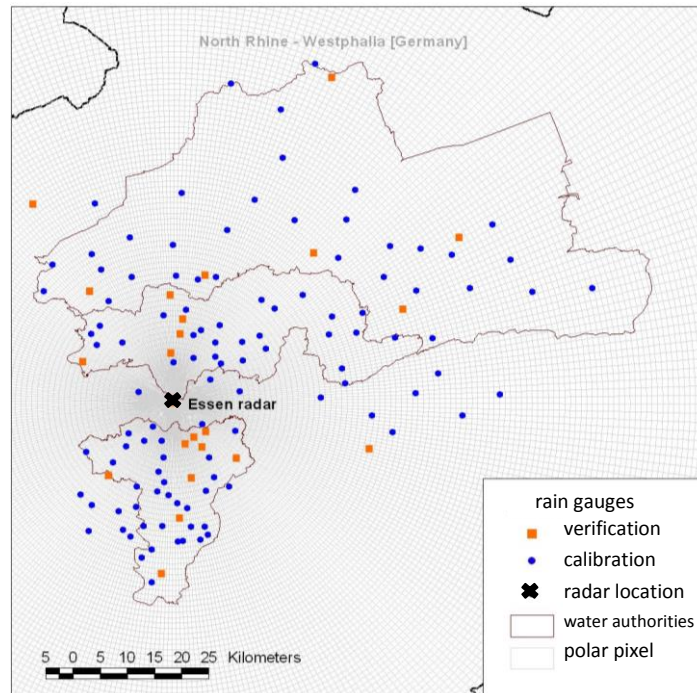


Figure 2: Investigated area with rain gauge locations

3.1 Data quality

Quality of radar data is variable in time and space. Intensity scans of radar Essen are corrupted by clutter and partial beam blockage. In order to enhance the data quality, different correction procedures for ground clutter, partial beam blockage and attenuation were carried out (Jessen at al., 2008).

For merging radar and rain gauge information, a good quality of rain gauge data is necessary. For this reason, rain gauge data was quality checked by comparing data from neighbouring stations. Periods containing potential measurement errors were excluded from further work.

3.2 Adjustment of radar data

Merging radar data with values from ground stations is a necessary step for radar-based quantitative precipitation estimation (Jessen at al., 2008). An adjustment procedure was carried out, generating daily factor fields based on corrected radar data and quality-checked rain gauges. The adjustment factors were calculated at the locations of the rain gauges and an interpolation with the factors from the four nearest stations was done, using the IDW (Inverse Distance Weighting) method.

Table 1: Evaluation parameters

	number of stations	number of investigated daily sums	raingauge sum [mm]	adjusted radar sum [mm]	factor raingauge/radar [-]
calibration stations					
correction + adjustment	112	38972	97306	100195	0.971
correction + interpolation + adjustment	112	38972	97306	100217	0.971
verification stations					
correction + adjustment	25	6864	17661	18859	0.936
correction + interpolation + adjustment	25	6864	17661	18528	0.953
all stations					
correction + adjustment	137	45836	114967	119054	0.966
correction + interpolation + adjustment	137	45836	114967	118746	0.968

4 Results

4.1 Visual comparison

An example of radar-derived daily rain from radar Essen is shown in Figure 1. On the left-hand side, the corrected and adjusted daily rain sum is displayed. The rain sum is calculated by a standard cumulation, assuming constant rain rates over the 5 min time intervals of the radar measurement. The additional effect of the 1 min temporal interpolation (right-hand side) is evident. The resulting structures seem plausible and clearly improved compared to the not-interpolated rain sum. Another example is given in Figure 4. In this example, the temporal interpolation also improves the rain sum and removes artificial extremes. However some artefacts of the cumulation are left. Here even a shorter interpolation time step than 1 min could be necessary. At days with low wind speed and little advection on the other hand, daily sums are nearly not changed by the temporal interpolation. A visual check of a number of days shows that mostly the interpolation with the 1 min time step brings good results.

4.2 Evaluation with rain gauge measurements

To evaluate overall results, one year of radar-derived daily rain sums are compared to rain gauge sums at 137 rain gauge locations. Radar-derived rain sums are corrected and adjusted using 112 rain gauge stations for the adjustment procedure, 25 stations are used for verification. An overview of the station and evaluation parameters is given in Table 1. In total, 45836 daily values were analysed whereof 20073 values have rain above 0.5 mm measured by the rain gauges. At most days the differences between radar-derived and rain gauge rain sums are small, both for calibration and verification stations. Differences above 3 mm are listed in Table 2. The number of daily differences above 3 mm is significantly decreased by temporal interpolation, both for calibration stations (-30%) and validation stations (-28%). For four classes of daily differences the results with and without temporal interpolation are shown in Figure 5. The temporal interpolation improves the results for all classes.

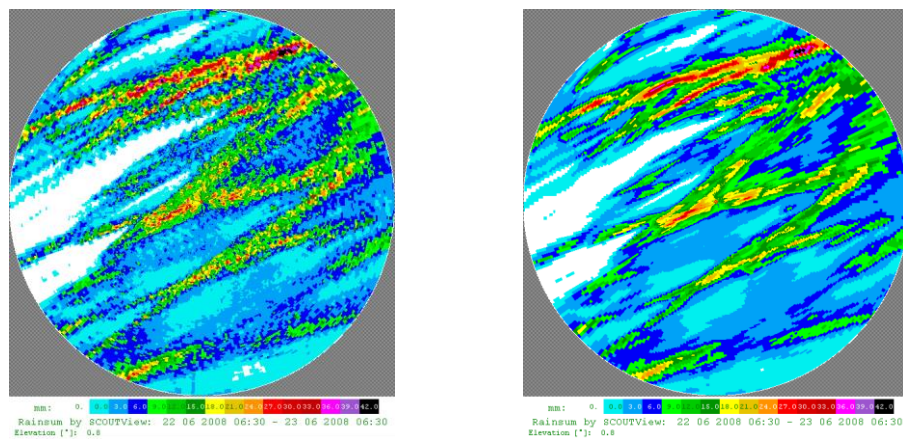


Figure 3: corrected (left) and corrected and temporal interpolated (right) radar sums of one day

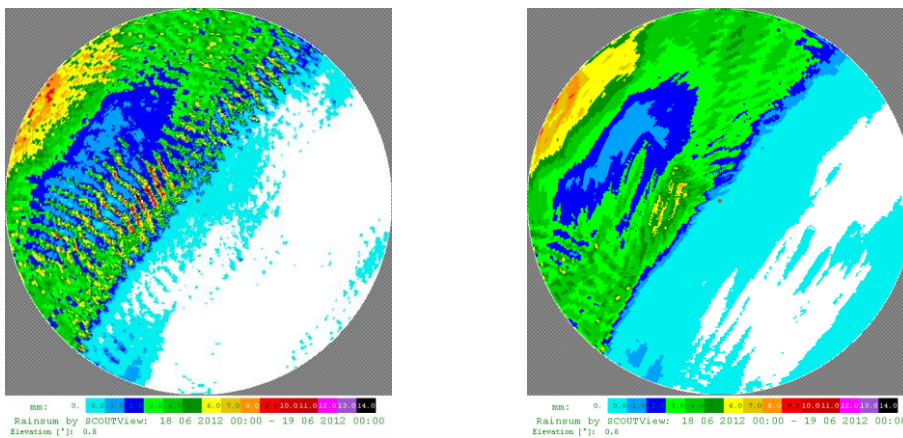


Figure 4: corrected (left) and corrected and temporal interpolated (right) radar sums of one day

Table 2: Criteria daily differences rain gauges – adjusted radar

	number of daily differences raingauge - adjusted radar				
	3 - 5	5 -10	10 - 20	>20	total
	[mm]	[mm]	[mm]	[mm]	
calibration stations					
correction + adjustment	43	12	2	0	57
correction + interpolation + adjustment	32	8	1	0	41
verification stations					
correction + adjustment	128	56	20	9	213
correction + interpolation + adjustment	93	34	17	6	150
all stations					
correction + adjustment	171	68	22	9	270
correction + interpolation + adjustment	125	42	18	6	191

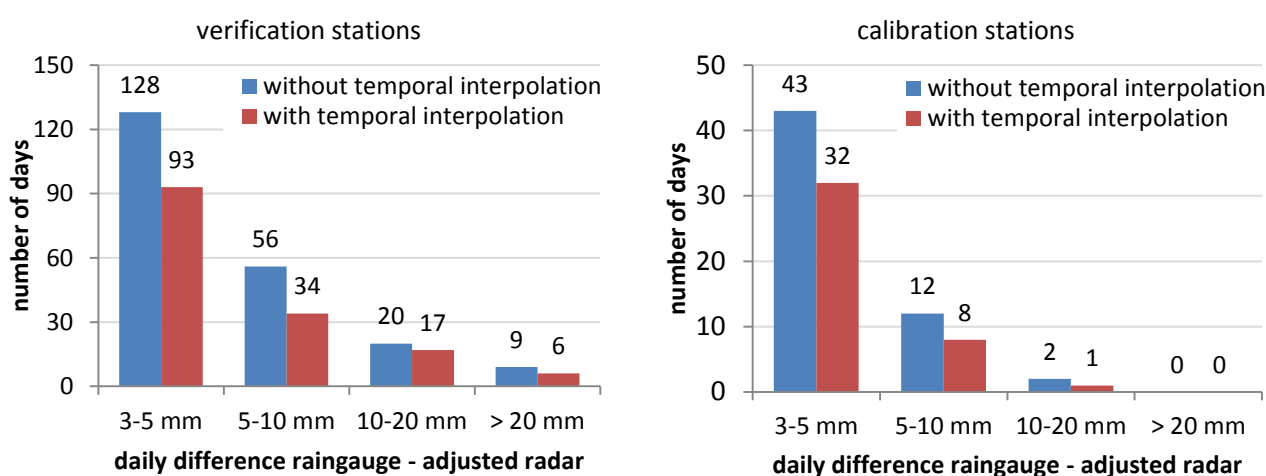


Figure 5: Daily differences of rain gauge and radar-derived daily sums for corrected and adjusted radar data with and without temporal interpolation at calibration (left) and verification stations (right).

5 Conclusion

The described temporal interpolation method clearly improves radar-derived rain sums. An evaluation of one year data from radar and rain gauges shows an improvement of almost 30% considering the number of radar – rain gauge differences above 3 mm. A visual comparison shows more homogeneous structures from daily rain sums calculated with temporal interpolation with artificial extremes and voids being removed. The described method can be used on polar grids keeping the original spatial resolution of radar scans, without losing information by mapping and remapping. The 1 min time step of the temporal interpolation is sufficient in most cases.

Thus the temporal interpolation is an important contribution to radar data processing. In particular it is an important preparation step for rain gauge based adjustment where minor location errors can deteriorate results considerably. Temporal interpolation on the original polar grid can also improve results of a subsequent compositing of several radars.

The described method is computationally not expensive and can also be used in real-time applications. Interpolated rain rates are then determined up to the last measurement interval. It is planned to include the temporal interpolation in operational processing with the software SCOUT in near future to improve real-time adjustment and QPE.

Acknowledgement

Thanks to Thomas Einfalt, Guido Lempio and Annemarie Jackisch for supporting the study and for giving helpful comments.

References

Anagnostou, E. N. and Krajewski, W. F. Real-time radar rainfall estimation. Part I: Algorithm formulation. *Journal of Atmospheric and Oceanic Technology* 16.2 - 1999 - pp. 189 - 197.

Ciach, G. J and Krajewski, W. F. and Anagnostou, E. N. and Baeck, M. L. and Smith, J. A. and McCollum, J. R., and Kruger, A. Radar rainfall estimation for ground validation studies of the Tropical Rainfall Measuring Mission. *Journal of Applied Meteorology*, 36(6) - 1997 - pp. 735-747.

Einfalt, T. and Lobbrecht, A. and Leung, K. and Lempio, G. Preparation and evaluation of a Dutch-German radar composite to enhance precipitation information in border areas. *Journal of Hydrologic Engineering*, 18(2) - 2012 - pp. 279-284.

Jessen M. and Einfalt T. Lessons learnt from the analysis of two years of weather radar data. *Proceedings ERAD - 2008* - ISSN 978-951-697-676-4

Tessendorf, A. and Einfalt, T. Ensemble radar nowcasts – a multi-method approach. *IAHS Publ.* 351. - 2012 - pp. 305-310.